Absorption Spectrum of Mn^{2+} Ions Doped in Zinc Thallium Sulphate Hexahydrate

J. Lakshmana Rao, M. Ramachandra Reddy, and S. V. J. Lakshman

Department of Physics, S. V. University, Tirupati – 517 502, India

The optical absorption spectrum of Mn^{2+} ions doped in zinc thallium sulphate hexahydrate has been studied at room and liquid nitrogen temperatures. The observed bands are assigned as transitions from the $^6A_{1g}(S)$ ground state to various excited quartet levels of Mn^{2+} ion in octahedral symmetry. The fine structure observed in the $^4T_{2g}(D)$ band is explained as due to spin-orbit interaction. All the observed band positions have been fitted with the parameters B, C, Dq and α.

1. Introduction

The optical absorption spectra of manganese complexes in octahedral and tetrahedral symmetry have attracted the attention of many theoretical and experimental investigators [1–7]. This is in part due to the richness of spectral details possible at low temperature and in part due to the uniqueness of the d^5 electronic configuration. The interesting feature of the Mn^{2+} complex is that a number of bands of this ion are observed in the visible and ultraviolet regions. Since no optical absorption studies of this ion doped in zinc thallium sulphate hexahydrate (ZTlSH) have been reported in literature, the authors have taken up these studies.

The crystal structure of Tutton salt (ZTlSH) is known to be monoclinic and contains two molecules in the unit cell, related by the space group $P2_{1/a}$ [8, 9]. The divalent ion is situated at the positions $(0, 0, 0)$ and $(\frac{1}{2}, \frac{1}{2}, 0)$ in the unit cell and is surrounded by a slightly distorted octahedron of six water molecules. Jain and Venkateswarlu [10] studied the electron paramagnetic resonance spectra of Mn^{2+} ions doped in zinc thallium sulphate hexahydrate and concluded that the Mn^{2+} ion enters the Tutton salt lattice in the divalent sites, forming magnetic $Mn(H_2O)_6^{2+}$ complexes. From angular variation studies they found that the crystal field symmetry at the Mn^{2+} site may be either orthorhombic or more probably lower.

2. Experimental

The crystals were grown at room temperature from an aqueous solution of zinc thallium sulphate hexahydrate to which a few mole percent of manganese sulphate were added. The crystals grown were clear and pale pink in colour. The spectra were recorded both at room and liquid nitrogen temperatures with a Cary 17 spectrophotometer.
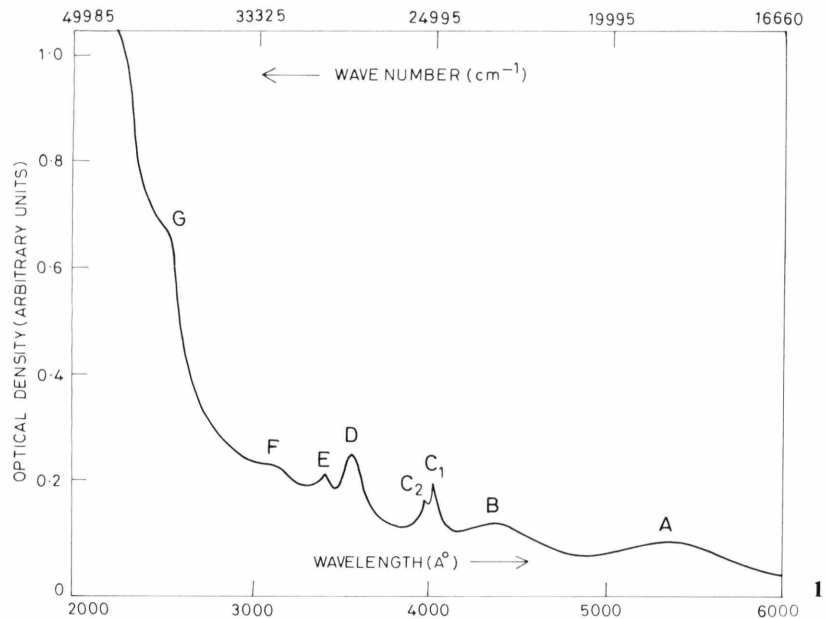
3. Results and Analysis

The spectra recorded at room and liquid nitrogen temperature are shown in Figs. 1 and 2, respectively.

Seven bands, (A–G) have been observed both at 300 K and 77 K. The bands A and B are broad. The band C is sharp, the bands D and F are moderately broad, the band E is moderately sharp and the band G appears as a shoulder. On cooling the crystal to liquid nitrogen temperature, the bands A and B showed red shifts while the bands F and G showed blue shifts. The band D exhibited structure at 77 K, while the band C exhibited structure both at 300 K and 77 K. The band E splits into two components E_1 and E_2 at 77 K.
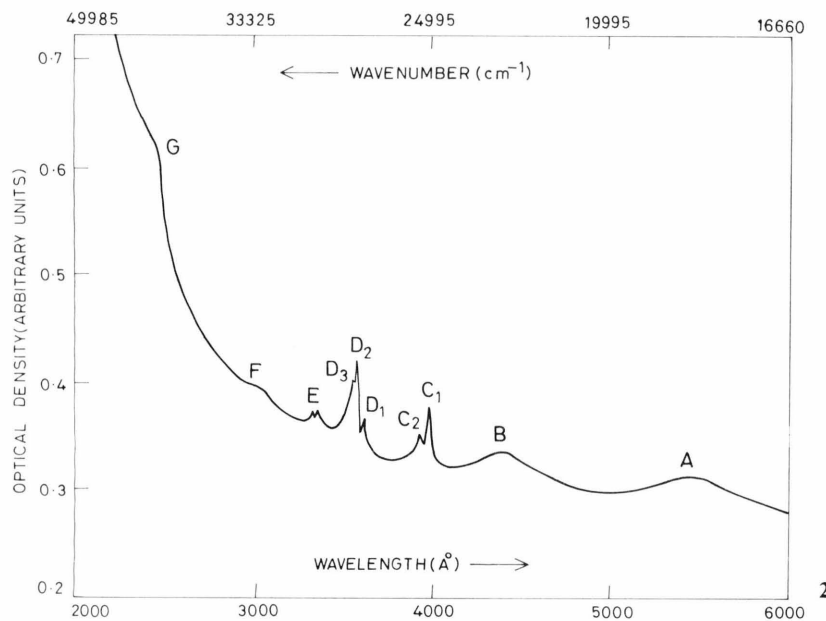
From the nature and position of the bands observed, they have been attributed to Mn^{2+} in octahedral symmetry. For the analysis of the spectrum being reported here, the local symmetry around Mn^{2+} will be taken as octahedral since the overall distortion in the octahedral symmetry around Mn^{2+} should be very small. Ligand field bands are sharp
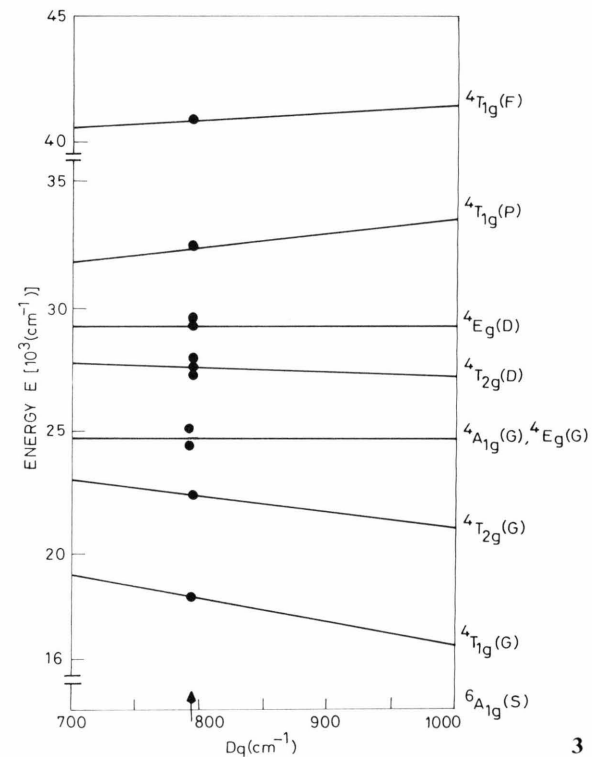
Fig. 3. Energy level diagram of Mn^{2+} in octahedral symmetry for $B = 800$ cm^{-1}, $C = 3050$ cm^{-1} and $\alpha = 76$ cm^{-1}. The observed band energies in the spectrum of Mn^{2+} in zinc thallium sulphate hexahydrate at 77 K are marked as solid circles at $Dq = 795$ cm^{-1}.

Fig. 1. Absorption spectrum of Mn^{2+} in zinc thallium sulphate hexahydrate at 300 K.

Fig. 2. Absorption spectrum of Mn^{2+} in zinc thallium sulphate hexahydrate at 77 K.

J. L. Rao *et al.* · Absorption Spectrum of Mn^{2+} Ions

Table 1. Observed and calculated energies and assignments for the bands of Mn^{2+} in zinc thallium sulphate hexahydrate. $B = 800$ cm^{-1}, $C = 3050$ cm^{-1}, $Dq = 795$ cm^{-1} and $\alpha = 76$ cm^{-1}.

Absorption peak	Observed at		Calculated	Transition from $^6A_{1g}$(S) to
	300 K cm^{-1}	77 K cm^{-1}	cm^{-1}	
A	18 650	18 375	18 385	$^4T_{1g}$(G)
B	22 720	22 540	22 515	$^4T_{2g}$(G)
[C_1]	24 790	24 835		$^4A_{1g}$(G)
			24 845	
[C_2]	24 900	25 120		^4E_g(G)
[D_1]		27 465		
[D_2]	27 770	27 730	27 640	$^4T_{2g}$(D)
[D_3]		27 885		
[E_1]	29 405	29 500	29 335	^4E_g(D)
[E_2]		29 620		
F	32 510	32 615	32 475	$^4T_{1g}$(P)
G	40 805	40 970	40 880	$^4T_{1g}$(F)

when the energy expressions for the transitions are independent of Dq, because the number of t_{2g} electrons is the same in both the excited and ground states (Ballhausen [11]). The sharp band C and the moderately sharp band E are therefore attributed to $^4A_{1g}$(G), ^4E_g(G) and ^4E_g(D) states, respectively, as their energy expressions are independent of Dq. The first two broad bands A and B are assigned to transitions $^6A_{1g}$(S) → $^4T_{1g}$(G) and $^6A_{1g}$(S) → $^4T_{2g}$(G), respectively. The bands D, F and G are assigned to transitions to $^4T_{2g}$(D), $^4T_{1g}$(P) and $^4T_{1g}$(F) states, respectively.

The Racah parameters B and C are evaluated for the 77 K spectrum using the following expressions given by Rao et al. [12]:

$$B = \frac{94\,\alpha + [49(E_2 - E_1)^2 - 768\,\alpha^2]^{1/2}}{49} \quad \text{and}$$

$$C = \frac{E_1 + E_2 - 27\,B - 26\,\alpha}{10},$$

where E_1 and E_2 are energies of the transitions $^6A_{1g}$(S) → $^4A_{1g}$(G) and $^6A_{1g}$(S) → ^4E_g(D), respectively.

The energy values for quartet electronic states have been calculated for different values of Dq with $B = 800$ cm^{-1}, $C = 3050$ cm^{-1} and $\alpha = 76$ cm^{-1} for the 77 K spectrum. A good fit of the experimentally observed band positions is obtained, as is seen from the graph in Fig. 3, for $Dq = 795$ cm^{-1}. The observed and calculated energies of the bands along with their assignments are given in Table 1.

4. Discussion

When the crystal is cooled to liquid nitrogen temperature, the bands $^6A_{1g}$(S) → $^4T_{1g}$(G) and $^6A_{1g}$(S) → $^4T_{2g}$(G) are shifted towards red by 275 cm^{-1} and 180 cm^{-1}, respectively. This red shift is in accordance with the theory since the corresponding energy levels have large negative slopes in the energy level diagram of the d^5 configuration [13]. On the other hand, the levels $^4T_{1g}$(P) and $^4T_{1g}$(F) showed a blue shift of 105 cm^{-1} and 165 cm^{-1}, since these levels have positive slopes.

The two states $^4A_{1g}$(G) and ^4E_g(G) are normally degenerate, but their degeneracy is often lifted by covalency in the crystal. According to the covalency model proposed by Stout [14], the removal of degeneracy can be explained by the differential expansion of (t_{2g}) and (e_g) orbitals. The relative order of the levels $^4A_{1g}$(G) and ^4E_g(G) has long been debated. According to Ferguson [15] and Lohr [16] any of the two could be lower. Extensive work of Ferguson et al. [17], for Mn^{2+}:$KMgF_3$ confirms that the band ^4E_g(G) lies lower than $^4A_{1g}$(G) by about 30 cm^{-1}. In the present work, similar conclusions may not be reached qualitatively from the following discussion. Since the ^4E_g(G) level is expected to be affected by configuration interaction with the ^4E_g(D) level, while the $^4A_{1g}$(G) is not affected, it is reasonable to assign the $^4A_{1g}$(G) level below the ^4E_g(G) level. Consequently, the $^4A_{1g}$(G) level is expected to be less affected compared to the ^4E_g(G) level by slight changes in the geometry and the metal-ligand bond distances. Considering all the above factors, the peak marked C_1 has been attributed to the transition $^6A_{1g}$(S) → $^4A_{1g}$(G) and the peak C_2 to the $^6A_{1g}$(S) → ^4E_g(G) transition.

Structure of the D Band

The D band assigned to the $^6A_{1g}$(S) → $^4T_{2g}$(D) transition is split at liquid nitrogen temperature into three components, D_1, D_2 and D_3, with maxima at 27 465 cm^{-1}, 27 730 cm^{-1} and 27 885 cm^{-1}, respectively. This band is expected to show fine structure at low temperature since this level is almost parallel to the ground level in the energy level diagram, and the same was reported by Stout [14], and Mehra et al. [18]. Several authors have reported spin-orbit splittings of the $^4T_{2g}$(D) level.

The $^4T_{2g}$(D) level splits under spin-orbit coupling as

$$\Gamma_8 \times \Gamma_{2g} = \Gamma_6 + \Gamma_7 + 2\Gamma_8.$$

Table 2. Energy parameters for the Mn^{2+} ion in various crystals.

Mn^{2+} ion in	Dq	B	C	Reference
Free ion	–	915	3235	[20]
MnF$_2$	750	840	3095	[14]
ZTlSH	795	800	3050	Present work
MnCl$_2$	770	684	3352	[21]
MnBr$_2$	680	669	3278	[21]
MnI$_2$	640	640	3136	[21]

First order splittings calculated from Lande's formula using fictitious $L' = 1$ are

$$E = 5a(\Gamma_7),\; 2a(\Gamma_8) \text{ and } -3a(\Gamma_6 + \Gamma_8),$$

where 'a' is a proportionality constant (Goode [19]). Γ_6 and Γ_8 are very close together, and hence one can expect three spin-orbit components with their spacing in the ratio of $3:5$. In the present investigation, the peaks D_1, D_2 and D_3 seem to be the spin-orbit components of the $^4T_{2g}(D)$ level. The separations $D_3 - D_2$ and $D_2 - D_1$ are in the ratio $155:265 \approx 3:5$, which agrees well with the first order splitting ratio.

Structure of the E Band

The simplest structure is observed in the $^4E_g(D)$ band shown in Fig. 2, which consists of two components E_1 and E_2 at liquid nitrogen temperature with maxima at 29 500 cm^{-1} and 29 620 cm^{-1}, respectively. The separation between the two observed peaks E_1 and E_2 is 120 cm^{-1}. This large splitting cannot be due to spin-orbit since the estimated spin-orbit components are spread over less than 40 cm^{-1} according to Mehra and Venkateswarlu [18]. Hence in all probability the splitting represents some vibrational frequency of the upper electronic state.

In the present investigation, a broad hump is observed in the ultraviolet region both at room and liquid nitrogen temperature, as shown in Fig. 1 and 2. This band marked G is assigned to the transition $^6A_{1g}(S) \rightarrow {}^4T_{1g}(F)$.

The energy parameters obtained in the present work are presented in Table 2 along with the energy parameters reported for Mn^{2+} in various crystals. From the table it is clear that the B value decreases in the order

$$F^- < H_2O < Cl^- < Br^- < I^-.$$

This confirms that in the present work the Mn^{2+} ions are surrounded by H$_2$O molecules. As compared with other compounds of the Mn^{2+} ion, considering spectrochemical series, the value of Dq obtained in the present work is also reasonable.

The interelectronic repulsion parameter B for free Mn^{2+} is 915 cm^{-1}. In the present work, the authors obtained B value equal to 800 cm^{-1}, and this suggests that the ionic bonding is greater in the complex. The ionic radius is 0.80 Å for Mn^{2+} and 0.74 Å for Zn^{2+}, and it is reasonable to assume that the Mn^{2+} ions can substitute the Zn^{2+} ions. From the observed optical absorption spectra, the authors conclude that Mn^{2+} ions substitute Zn^{2+} ions and the site symmetry is distorted octahedral.

5. Acknowledgements

[1] J. Ferguson, Progress in Inorganic Chemistry, ed. S. J. Lippard, Interscience, New York **12**, 159 (1970).
[2] E. Konig, R. Schnakig, and S. Kremer, Z. Naturforsch. **29a**, 419 (1974).
[3] D. Curie, C. Barthou, and B. Canny, J. Chem. Phys. **61**, 3048 (1974).
[4] M. Vala, J. C. Rivoal, and J. Badoz, Molec. Phys. **30**, 1325 (1975).
[5] J. P. Srivastava, J. Phys. Chem. Solids **36**, 727 (1975).
[6] B. Ghosh and R. K. Mukherjee, Phys. Stat. Sol(b) **106**, 699 (1981).
[7] K. Purandar, J. L. Rao, and S. V. J. Lakshman, Acta. Phys. Slov. **34**, 195 (1984).
[8] R. W. G. Wyckoff, Crystal Structures, Interscience, New York **3**, 821 (1965).
[9] A. E. H. Tutton, Crystallography and Practical Crystal Measurement, Today and Tomorrow's Book-Agency, New Delhi 1964, p. 258.
[10] V. K. Jain and P. Venkateswarlu, J. Phys. (C) Sol. State Phys. **12**, 865 (1979).
[11] C. J. Ballhausen, Introduction to Ligand Field Theory, McGraw Hill, New York 1962.
[12] J. L. Rao and K. Purandar, Solid State Commun. **37**, 983 (1981).
[13] Y. Tanabe and S. Sugano, J. Phys. Soc. Japan **9**, 753 (1954).
[14] J. W. Stout, J. Chem. Phys. **31**, 709 (1959).
[15] J. Ferguson, Australian J. Chem. **21**, 307 (1968).
[16] L. L. Lohr, Jr., J. Chem. Phys. **45**, 3611 (1966).
[17] J. Ferguson, E. R. Krausz, and H. J. Guggenheim, Molec. Phys. **27**, 577 (1974).
[18] A. Mehra and P. Venkateswarlu, J. Chem. Phys. **47**, 2334 (1967).
[19] D. H. Goode, J. Chem Phys. **43**, 2830 (1965).
[20] C. Moore, Nat. Bur. Stand (U.S.) Circ. No. **467**, 2 (1952).
[21] W. Van Erk and C. Haas, Phys. Stat. Sol(b) **70**, 517 (1975).